



## Article

# Polymerization of Solid-State Aminophenol to Polyaniline Derivative Using a Dielectric Barrier Discharge Plasma

Ketao Chen, Meijuan Cao, Eileen Feng, Karl Sohlberg  and Hai-Feng Ji 

Department of Chemistry, Drexel University, Philadelphia, PA 19104, USA; kc944@drexel.edu (K.C.); 13693156432@126.com (M.C.); eileenfeng123@hotmail.com (E.F.); kws24@drexel.edu (K.S.)

\* Correspondence: hj56@drexel.edu; Tel.: +1-215-895-2562; Fax: +1-215-895-1265

Received: 19 September 2020; Accepted: 24 October 2020; Published: 30 October 2020



**Abstract:** We present a method to prepare polyaminophenol from solid-state aminophenol monomers using atmospheric dielectric barrier discharge (DBD) plasma. The polymerizations of *o*-aminophenol and *m*-aminophenol are studied. The polymers were analyzed via Fourier-Transform infrared spectroscopy (FTIR) and ultraviolet-visible (UV-vis) spectroscopy. The kinetics of the polymerization reactions were investigated by using UV-vis and the polymerization was found to be first-order for both *o*-aminophenol and *m*-aminophenol. The resulting polymer film exhibits a conductivity of  $1.0 \times 10^{-5}$  S/m for poly-*o*-aminophenol (PoAP) and  $2.3 \times 10^{-5}$  S/m for poly-*m*-aminophenol (PmAP), which are two orders more conductive than undoped ( $\sim 10^{-7}$  S/m) polyaniline (PANI). The PoAP has a quinoid structure and the PmAP has an open ring keto-derivative structure. The process provides a simple method of preparing conductive polyaminophenol films.

**Keywords:** polymer synthesis; non-thermal plasma; polymerization; aminophenol; conductive polymer

## 1. Introduction

Conductive polymers like polyacetylene, polypyrrole, polyaniline, polythiophene, and their derivatives have been widely studied [1]. The conductive polymers have prospective applications for energy storage devices, batteries, smart windows, biosensor and surface coatings, etc. [2]. The advantages of using conductive polymer materials for such applications include their flexibility, versatility, light weight, etc. [3].

Among conductive polymers, polyaniline (PANI) is widely studied because it is easily synthesized, environmentally stable and widely applicable [4]. Its processability is better than that of other conductive polymers [5]. The processing of PANI is however still an issue since PANI has low solubility in most solvents. One way to solve this problem is to polymerize monomers that have substituent groups, such as aniline derivatives. Aniline is commonly derivatized by *ortho*- or *meta*-substitution with -OH, -OCH<sub>3</sub>, -Cl, -CH<sub>3</sub>, etc. [6].

Aminophenols are derivatives of anilines that contain *ortho*-, *meta*- or *para*-substituted -OH groups [7]. Chemical oxidative polymerization [8] and electrochemical anodic oxidation [9] are popular techniques to synthesize polyaminophenols. In chemical oxidative polymerization, a monomer is generally combined with an acid and an oxidant in a suitable polymerization medium. Ammonium persulfate (APS) [1], copper bromide [10], iron chloride [2], and hydrogen peroxide [11] can be used as oxidants. Aqueous, organic or an aqueous/organic solvent mixture (miscible or immiscible) may be used as the polymerization medium. For electrochemical polymerization, monomers are dissolved in the solution and polymer materials formed by electrochemical oxidations and reductions.

Recently, printable electronics have attracted a lot of attention due to the low cost and convenience of this fabrication strategy [12]. Most of the conductive materials used for printing are inorganic

materials. Printing a conductive polymer, such as polyaniline or polyaminophenol, is difficult since these materials don't dissolve well in many solvents. One solution is to print the monomers and polymerize the printed pattern of the monomers later. However, neither of the above two methods can be used to polymerize solid monomer patterns since the solvents will dissolve the monomer patterns on a surface.

In this study, we demonstrate that a film of solid aminophenol can be polymerized on exposure to a dielectric barrier discharge (DBD) plasma without any additives and solvents. DBD is a plasma under room temperature and atmospheric pressure. A high voltage is applied between two electrodes and at least one electrode is insulated to assure no electron flow between the electrodes. Thus, the DBD plasma is safer to use than thermal plasma [13,14]. The DBD device can be made at a low cost as a device that is similar to a UV handheld device [15]. Other advantages include less pollution to the environment, shorter treatment time etc. [16,17]. The air-plasma contains reactive oxygen species and reactive nitrogen species (ROS and RNS) that can initiate the polymerization reaction. Overall, the DBD polymerization method is simple and straightforward. The formation and the characterization of the polymers, and the reaction rate have been investigated in the present study.

## 2. Experiments and Materials

2-aminophenol (o-aminophenol, >98%, TCI, Tokyo, Japan), 3-aminophenol (m-aminophenol, 98%, Aldrich, St. Louis, MO, USA), and ethanol (Fisher, Hampton, NH, USA) were used as received. To prepare an aminophenol thin film, 20 mg of monomer was dissolved in 0.1 mL of ethanol. The solution was drop-coated across a 10  $\mu\text{m}$  gap between two Au electrodes supported by a Si/SiO<sub>2</sub> wafer (Figure 1). The aminophenol-coated wafer was then treated with DBD in the atmospheric environment for 3 or 4 min until no further change was observed from on UV spectra. The DBD air plasma was generated using a setup reported previously [17]. Briefly, the size of the copper DBD electrode was 38 mm  $\times$  64 mm and it is covered with an 1-mm-thick glass slide. The resistance, dielectric constant, and dielectric strength of the glass slide are 1015  $\Omega$ , 4.6, and 30 kV/mm, respectively. The input energy was 10 mJ/pulse. The frequency of the power supply was from 500 Hz to 1.5 kHz with a max amplitude of 20 kV magnitude. The voltage and frequency of the plasma set-up were 11.2 kV ( $R = 75 \Omega$ ) and 1 kHz, respectively, for all the experiments [17]. The plasma discharge gap was 5 mm and the temperature is at 25  $^{\circ}\text{C}$ .

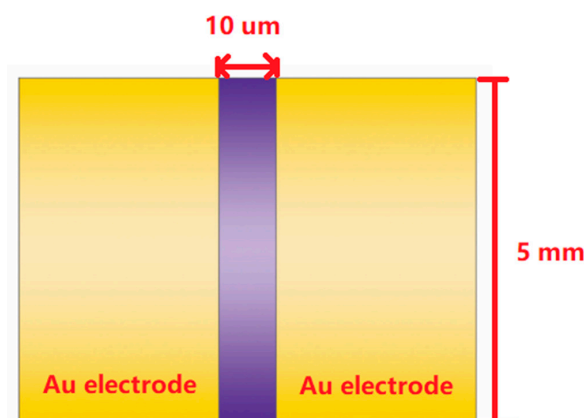


**Figure 1.** Scheme of films on substrates between the electrodes used in this work.

A Spectrum One FT-IR Spectrometer (PerkinElmer, Waltham, MA, USA) was used to obtain the Fourier Transform-Infrared (FT-IR) spectra of the samples before and after plasma polymerization. FTIR sampling was performed by attenuated total reflection (ATR) over the range 650  $\text{cm}^{-1}$  to 4000  $\text{cm}^{-1}$  with a resolution of 4  $\text{cm}^{-1}$ . The kinetics of plasma polymerization was investigated with a 8453 UV-vis spectrometer (Hewlett-Packard, Palo Alto, CA, USA). The background FTIR and UV-Vis spectra were collected on a gold substrate and high-density polyethylene substrate, respectively. The sample

coated on substrates was exposed to the plasma for different time intervals, and UV-vis spectra were collected immediately after the plasma treatment at room temperature. The conductivity of the polymer films was measured using a 2636A potential station (Keithley, Cleveland, OH, USA) with a two-probe method.

### 3. Results and Discussion

#### 3.1. *o*-Aminophenol (*o*AP, 2-Aminophenol)

##### 3.1.1. Infrared Spectra

It is commonly known that poly(*o*-aminophenol) (PoAP) is a ladder polymer with a structure like polyphenoxazine (Figure 2a) or an open-chain structure (Figure 2b) [1,2]. Oxidation of PoAP leads to the quinoid structure (Figure 2c) or the keto structure (Figure 2d) [18–20].

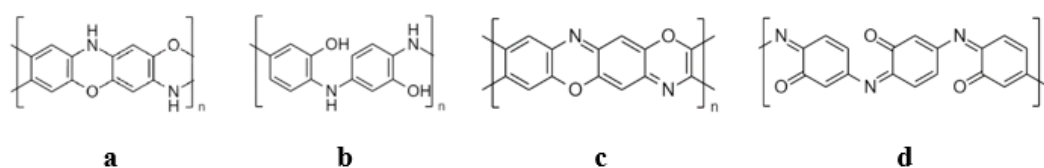


**Figure 2.** Various PoAP structures: (a) ladder-like. (b) open-chain. (c) quinoid structure. (d) keto form.

FTIR was used to confirm the polymerization of *o*AP after the plasma treatment. The peak values and their assignments are listed in Table 1. Bicak et al. [10], suggested that in the *o*AP monomer, the peak at  $1400\text{ cm}^{-1}$  could be due to a C-O-H deformation vibration, Figure 3 Left. This peak disappears after polymerization, and new peaks at  $1050$ ,  $1110$ , and  $1230\text{ cm}^{-1}$  emerge, which confirms the presence of a C-O-C linkage. According to the FTIR spectra of PoAP synthesized by Kunimura [9], the peak at  $1639\text{ cm}^{-1}$  is attributed to the C=N stretching. Table 1 shows that the PoAP prepared from DBD plasma in our work contains a C=O bond, a C-O-C linkage, a C=N bond, a C-N bond, and that the N-H and O-H stretch motions from the monomers are absent, suggesting the structure of our PoAP is the quinoid structure.

**Table 1.** IR peaks (unit  $\text{cm}^{-1}$ ) of PoAP in literature and our present work.

Functional Groups	This Work	Quinoid [1,9]	Keto [9,10]
C=O, carbonyl group stretching	n/a	n/a	1670
C=N, stretching	1639	1645	n/a
C=C, stretching vibration	1460, 1600	1430–1605	1450, 1590
C-N, stretching of aromatic ring	1281	1284	n/a
C-O-C, stretching vibration	1050, 1110, 1230	1050, 1112, 1235	1050, 1235

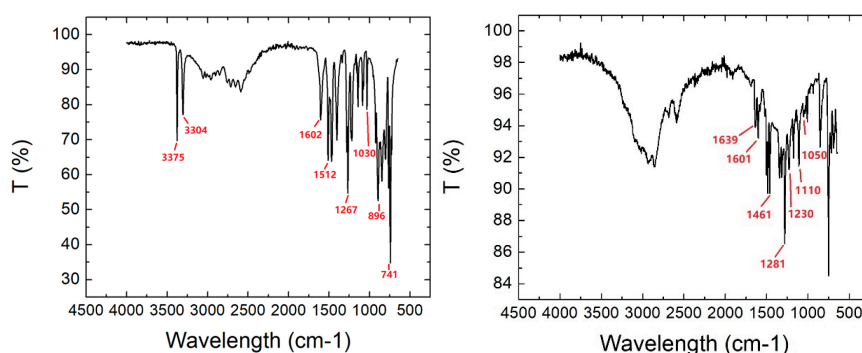


**Figure 3.** FTIR spectrum of *o*AP before (left) and after (right) the plasma treatment.

### 3.1.2. Kinetic Study Using UV-vis Spectra of the Film

To gain insight into the kinetics of the polymerization reaction, UV spectra were measured at different times during the plasma treatment. To prepare a polyaminophenol thin film, 20 mg of monomer was dissolved in 0.1 mL of ethanol. The solution was spin-coated on a high-density polyethylene substrate at 750 rpm over one minute for five times with an equal aliquot of 20  $\mu\text{L}$  each time. The air-plasma treated films were immediately analyzed using UV-vis. The UV-vis absorbance results for PoAP are shown below (Figure 4).

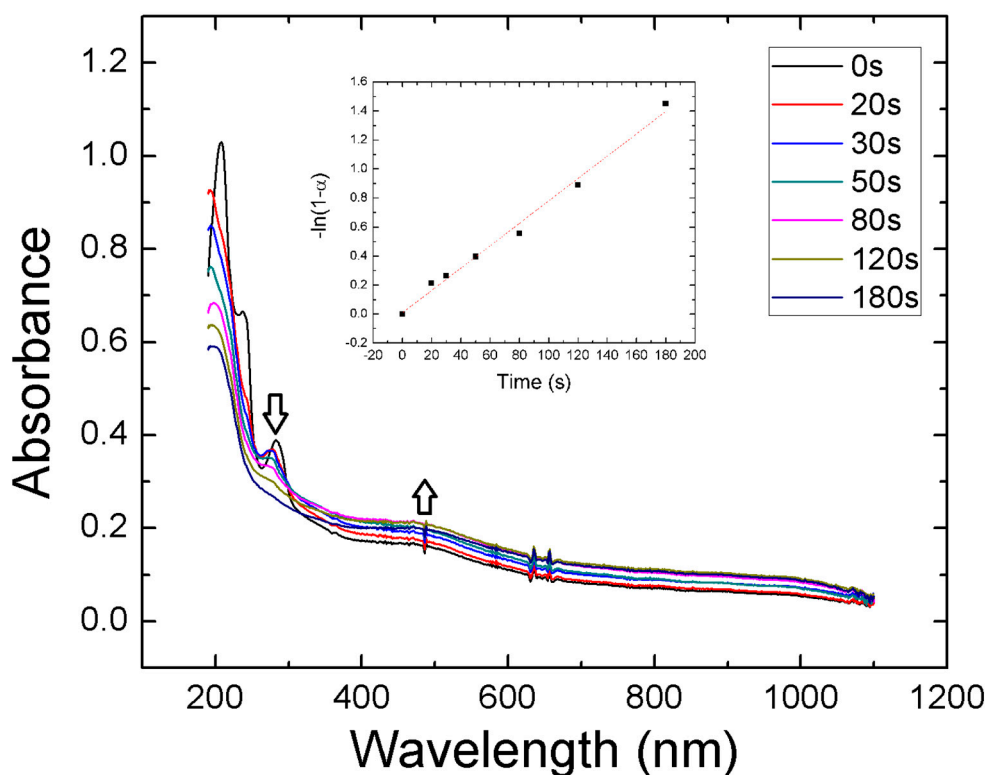


**Figure 4.** UV-visible absorbance of o-aminophenol films on a high-density polyethylene substrate treated with DBD for different durations of time. Graph plotted according to the solid-state reaction for the first order models at 283 nm vs. time. The arrows show the direction of intensity changes of the peaks at 490 nm and 283 nm during the plasma treatment.

As this is a solid-state polymerization, the kinetics of the polymer-producing reaction were studied according to the converted fraction of the monomer [21,22]. The reaction order was determined by applying for zero order, first order, and second order solid-state reaction models, with first-order producing the best overall fit.

The PoAP film shows an increase in absorbance at 490 nm upon polymerization, which is attributed to the  $\pi$ - $\pi^*$  transition. The associated orbitals are mostly related to the oxidized units [23]. The peak at 283 nm decreased during the plasma treatment and eventually disappeared entirely. The absorbance at 283 was therefore used to calculate the conversion percentage of the monomer,  $\alpha = (I_t - I_0)/(I_{\text{final}} - I_0)$ . The reaction rate and rate constants are then determined according to solid-state kinetic models reported by Khawam [23]. Figure 4 shows that the relationship between the conversion of percentage and the DBD treatment time is well-fitted by the model  $[-\ln(1 - \alpha) = kt]$ , which indicates the polymerization reaction follows first-order kinetics.

### 3.1.3. Conductivity of the Film after Plasma Treatment

When measuring conductivity, a silicon wafer coated with two gold electrodes was used. The two electrodes are separated by a gap 10  $\mu\text{m}$  wide and 5 mm long (see Figure 1). To prepare a polyaminophenol thin film, 20 mg of monomer was dissolved in 0.1 mL of ethanol. The solution was spin-coated on the wafer at 750 rpm over one minute for five times with an equal aliquot of 20  $\mu\text{L}$  each time. The samples were treated under plasma in the atmospheric environment for 10 min. The I-V curve of the PoAP was measured with a Keithley 2636A source meter using the two electrodes method (Figure 5). The conductivity was found to be  $1 \times 10^{-5}$  S/m.

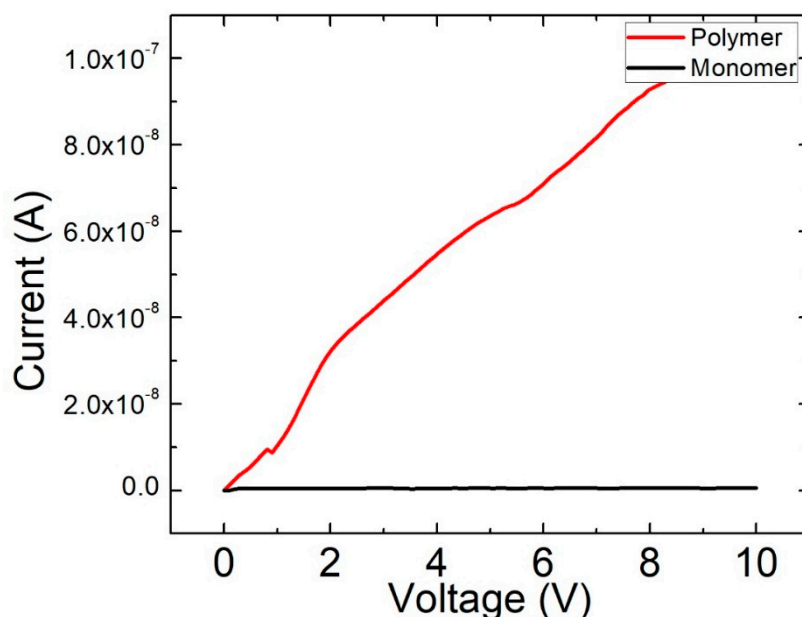


Figure 5. Conductivity of poly(o-aminophenol) film after plasma treatment.

## 3.2. *m*-Aminophenol (*m*-AP, 3-Aminophenol)

### 3.2.1. Infrared Spectra

For poly(*m*-aminophenol) (PmAP), there are two proposed structures. An open-ring structure (Figure 6a) [24], a complex structure (Figure 6b) [7], and a linear structure (Figure 6c) [25].

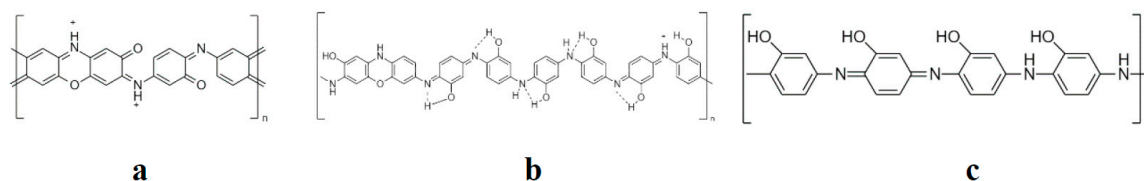


Figure 6. Various PmAP structures: (a) open-ring structure. (b) complex structure. (c) linear structure.

FTIR spectra of mAP before (left) and after (right) plasma treatment are shown in Figure 7. Peaks at 1041, 1220, and 1289  $\text{cm}^{-1}$  have been attributed to the C-O stretching and the C-O-C ether linkage [4]. The C=O stretching peak appears at 1697  $\text{cm}^{-1}$ . The sharp peak at 1601  $\text{cm}^{-1}$  is thought to be due to the C=N stretching in the quinoid rings [7]. Other characteristic peaks of PmAP are described in Table 2, clearly indicating that the PmAP fabricated in this work possesses an open ring keto derivative (Figure 6a).

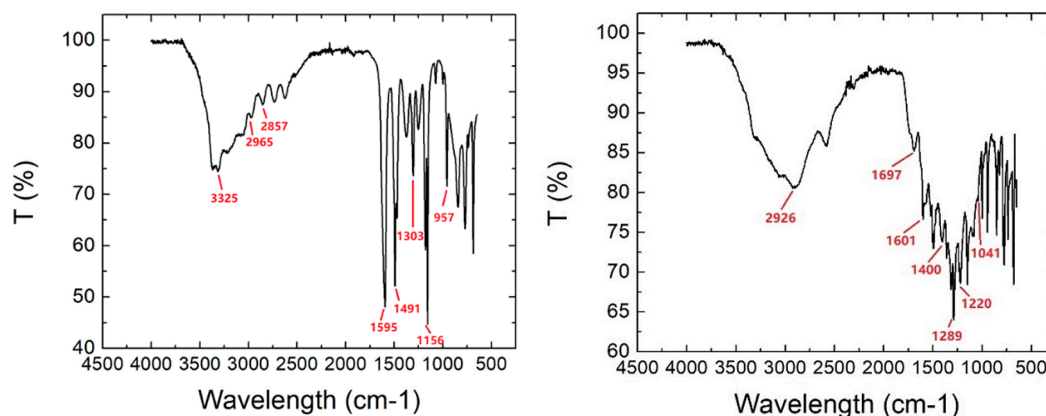


Figure 7. FTIR spectrum of mAP before (left) and after (right) plasma treatment.

Table 2. IR peaks (unit  $\text{cm}^{-1}$ ) of PmAP in literature and our present work.

	This Work	Ladder [24]	Complex [7]	Linear [25]
C-H, aromatic	2926	2930	-	2924
C=O, carbonyl group stretching	1697	1691	-	-
-N=C, stretching	1601	1593	1610	1615
C-O, stretching	1220, 1289	1234, 1288	-	1265
C-O-C, stretching vibration	1041	1026, 1195	1140	-

### 3.2.2. Kinetic Study Using UV-vis Spectra of the Film

For *m*-aminophenol, the PmAP film shows increasing absorbance from 300 nm to 590 nm, which results from the formation of a conjugated double bond (Figure 8). We used the absorbance at 319 nm to calculate the conversion percentage of the polymer,  $\alpha = (I_t - I_0)/(I_{\text{final}} - I_0)$ . Similar to the polymerization of oAP, this polymerization reaction also follows first-order kinetics. The rate constant is  $0.009 \text{ s}^{-1}$ , slightly larger than that found for oAP,  $0.008 \text{ s}^{-1}$ .

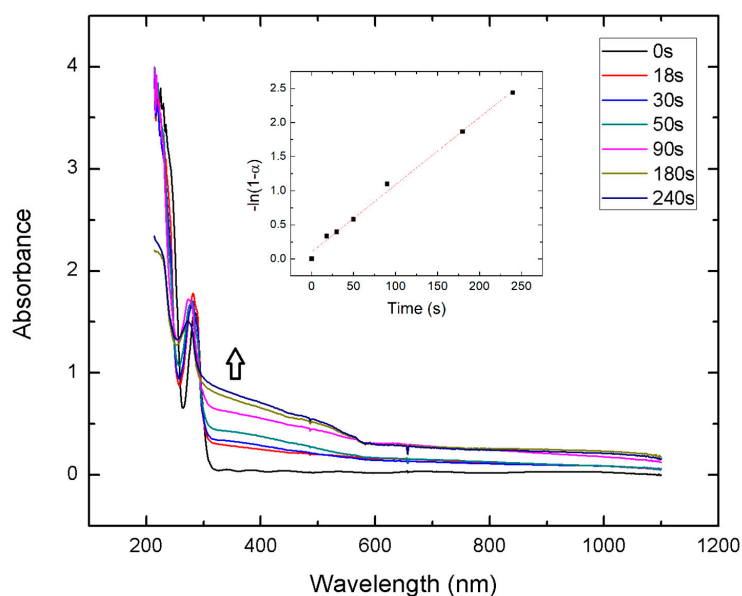


Figure 8. UV-visible absorbance of *m*-aminophenol films on a high-density polyethylene substrate treated with DBD. The arrow shows the direction of intensity changes of the peak at 319 nm during the plasma treatment.



### 3.2.3. Conductivity of the Film after Plasma Treatment

The conductivity of a PmAP film was also measured on a wafer coated with two gold electrodes. The I-V curve of PmAP was measured with a Keithley 2636A source meter (Figure 9) and the conductivity found to be  $2.3 \times 10^{-5}$  S/m, which is slightly higher than that of PoAP,  $1 \times 10^{-5}$  S/m.

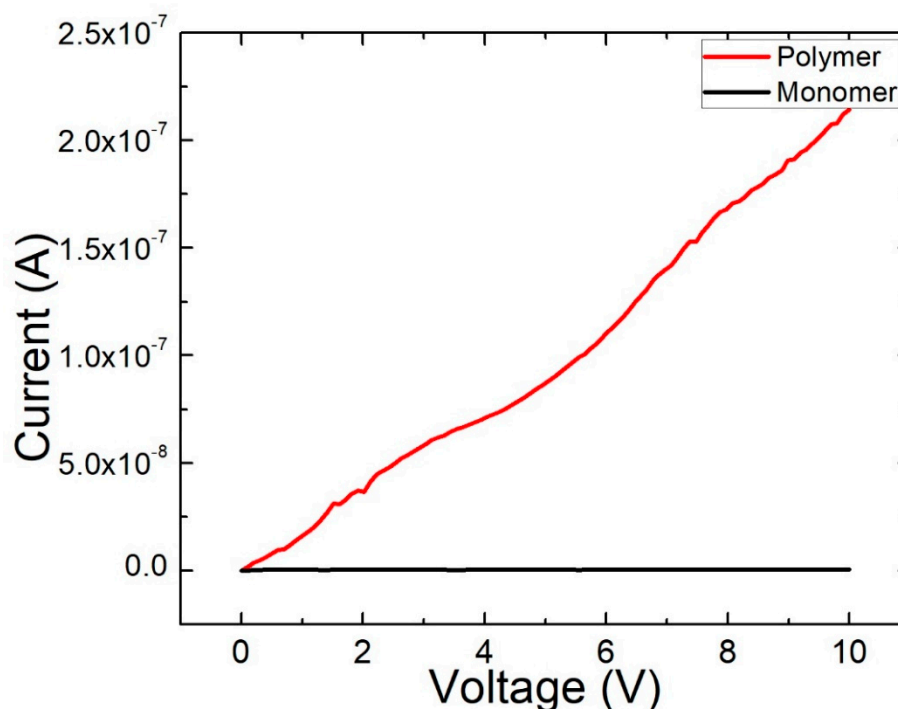


Figure 9. Conductivity of *m*-aminophenol film after plasma treatment.

## 4. Conclusions

Our work shows the plasma polymerization of *o*-aminophenol and *m*-aminophenol films directly with DBD plasma. Characterization by FTIR and UV-Vis supports the conclusion that polymerization has taken place. The conductivity of the thin polymer thin film is also measured and found to be on the order of  $1 \times 10^{-5}$  S/m for both materials and the conductivity of the PoAP is slightly higher than that of PmAP. The DBD polymerization method is therefore shown to be able to successfully synthesize conductive polymers in situ. The doping experiments, such as with HCl or NaOH, would be a desirable future target to establish whether the transport properties can be tuned. The PoAP has a quinoid structure and the PmAP has an open ring keto derivative structure. The effect of the position of the amino group on the performance of the two films will be studied and reported in due future. Exploration of the relationship between the reaction rate and plasma power could also be studied to establish the practicality of this approach for commercial application. The method will expand the applications of DBD, especially for the in situ synthesis of conductive polymers. The monomer may be soaked in any porous structure, such as paper, fiber, sponge, etc. Exposure these objects to DBD will convert them to be conductive for various applications.

**Author Contributions:** K.C. and H.-F.J. conceived and designed the experiments; K.C., M.C. and E.F. performed the experiments and analyzed the data; K.C., H.-F.J. and K.S. have contributed to writing and editing of the paper. All authors have read and agreed to the published version of the manuscript.

**Funding:** This research received no external funding.

**Acknowledgments:** This research was supported by the Drexel's ExCITE Center seed grant.

**Conflicts of Interest:** The authors declare no conflict of interest.

## References

1. Ghanem, M.A. Development of conducting poly(o-aminophenol) film and its capacitance behavior. *Int. J. Electrochem. Sci.* **2016**, *9*, 9987–9997. [\[CrossRef\]](#)
2. Al-Hossainy, A.F.; Zoromba, M.S.; Abdel-Aziz, M.H.; Bassyouni, M.; Attar, A.; Zwawi, M.; Abd-Elmageed, A.A.I.; Maddah, H.A.; Ben Slimane, A. Fabrication of heterojunction diode using doped-poly (ortho-aminophenol) for solar cells applications. *Phys. B Condens. Matter* **2019**, *566*, 6–16. [\[CrossRef\]](#)
3. Gowariker, V.R.; Viswanathan, N.V.; Sreedhar, J. *Polymer Science*, 1st ed.; New Age Publication (P) Ltd.: New Delhi, India, 2005; pp. 230–245.
4. Madhankumar, A.; Rajendran, N. Poly(m-phenylenediamine-co-o-aminophenol) coatings on mild steel: Effect of comonomers feed ratio on surface and corrosion protection aspects. *Prog. Org. Coat.* **2013**, *76*, 1445–1453. [\[CrossRef\]](#)
5. Syed, A.A.; Dinesan, M.K. Review: Polyaniline—A novel polymeric material. *Talanta* **1991**, *38*, 815–837. [\[CrossRef\]](#)
6. Dao, L.H.; Leclerc, M.; Guay, J.; Chevalier, J.W. Synthesis and characterization of substituted poly(anilines). *Synth. Met.* **1989**, *29*, 377–382. [\[CrossRef\]](#)
7. Gopalsamy, T.; Gopalswamy, M.; Gopichand, M.; Raj, J. Poly meta-aminophenol: Chemical synthesis, characterization and ac impedance study. *J. Polym.* **2014**, 1–11. [\[CrossRef\]](#)
8. Kar, P.; Behera, A.K.; Adhikari, B.; Pradhan, N.C. Optimization for the chemical synthesis of conducting poly (m-aminophenol) in HCl using ammonium persulfate. *High Perform. Polym.* **2010**, *22*, 428–441. [\[CrossRef\]](#)
9. Kunitura, S.; Ohsaka, T.; Oyama, N. Preparation of thin polymeric films on electrode surfaces by electropolymerization of o-aminophenol. *Macromolecules* **1988**, *21*, 894–900. [\[CrossRef\]](#)
10. Bicak, T.C.; Soylemez, S.; Buber, E.; Toppare, L.; Yagci, Y. Poly(o-aminophenol) prepared by Cu(ii) catalyzed air oxidation and its use as a bio-sensing architecture. *Polym. Chem.* **2017**, *8*, 3881–3888. [\[CrossRef\]](#)
11. Ivanov, V.; Zhuzhel'skii, D.; Malev, V. Comparison of properties of aniline and o-aminophenol polymers obtained using hydrogen peroxide. *Russ. J. Electrochem.* **2008**, *44*, 1204–1211. [\[CrossRef\]](#)
12. Neuvo, Y.; Ylönen, S. *Bit Bang: Rays to the Future*; Helsinki University: Helsinki, Finland, 2010.
13. Hegemann, D.; Nisol, B.; Gaiser, S.; Watson, S.; Wertheimer, M.R. Energy conversion efficiency in low and atmospheric-pressure plasma polymerization processes with hydrocarbons. *Phys. Chem. Chem. Phys.* **2019**, *21*, 8698–8708. [\[CrossRef\]](#) [\[PubMed\]](#)
14. Hegemann, D.; Nisol, B.; Watson, S.; Wertheimer, M.R. Energy conversion efficiency in low- and atmospheric-pressure plasma polymerization processes, Part II: HMDSO. *Plasma Chem. Plasma Process.* **2016**, *37*, 257–271. [\[CrossRef\]](#)
15. Mun, M.K.; Jang, Y.J.; Kim, J.E.; Yeom, G.Y.; Kim, D.W. Plasma functional polymerization of dopamine using atmospheric pressure plasma and a dopamine solution mist. *RSC Adv.* **2019**, *9*, 12814–12822. [\[CrossRef\]](#)
16. Liu, S.; Liu, D.; Pan, Z. The effect of polyaniline (PANI) coating via dielectric-barrier discharge (DBD) plasma on conductivity and air drag of polyethylene terephthalate (PET) yarn. *Polymers* **2018**, *10*, 351. [\[CrossRef\]](#) [\[PubMed\]](#)
17. Chen, K.; Cao, M.; Qiao, Z.; He, L.; Wei, Y.; Ji, H.-F. Polymerization of solid-state 2,2'-bithiophene thin film or doped in cellulose paper using DBD plasma and its applications in paper-based electronics. *ACS Appl. Polym. Mater.* **2020**, *2*, 1518–1527. [\[CrossRef\]](#)
18. Ohsaka, T.; Watanabe, T.; Kitamura, F.; Oyama, N.; Tokuda, K. Electrocatalysis of O<sub>2</sub> reduction at poly(o-phenylenediamine)- and poly(o-aminophenol)-coated glassy carbon electrodes. *J. Chem. Soc. Chem. Commun.* **1991**, 1072. [\[CrossRef\]](#)
19. Zhang, A.Q.; Cui, C.Q.; Chen, Y.Z.; Lee, J.Y. Synthesis and electrochromic properties of poly-o-aminophenol. *J. Electroanal. Chem.* **1994**, *373*, 115–121. [\[CrossRef\]](#)
20. Tucceri, R. Poly(o-aminophenol) as material of biosensors. *Research* **2014**, *1*, 884. [\[CrossRef\]](#)
21. Cai, J.; Liu, R. Kinetic analysis of solid-state reactions: A general empirical kinetic model. *Ind. Eng. Chem. Res.* **2009**, *48*, 3249–3253. [\[CrossRef\]](#)
22. Pérez-Maqueda, L.A.; Criado, J.M.; Sánchez-Jiménez, P.E. Combined kinetic analysis of solid state reactions: A powerful tool for the simultaneous determination of kinetic parameters and the kinetic model without previous assumptions on the reaction mechanism. *J. Phys. Chem. A* **2006**, *110*, 12456–12462. [\[CrossRef\]](#)



23. Khawam, A.; Flanagan, D.R. Solid-state kinetic models: Basics and mathematical fundamentals. *J. Phys. Chem. B* **2006**, *110*, 17315–17328. [[CrossRef](#)]
24. Behera, A.K.; Adhikari, B.; Kar, P. Synthesis of processable conducting poly(m-aminophenol) having structure like keto derivative of polyaniline. *Polym. Sci. Ser. B* **2015**, *57*, 159–166. [[CrossRef](#)]
25. Dinç, C.Ö.; Yalçınkaya, S.; Altuntaş, H.; Çolak, N. Synthesis and characterization of poly(m-aminophenol)-succinat. *Des. Monomers Polym.* **2014**, *17*, 629–636. [[CrossRef](#)]

**Publisher’s Note:** MDPI stays neutral with regard to jurisdictional claims in published maps and institutional affiliations.



© 2020 by the authors. Licensee MDPI, Basel, Switzerland. This article is an open access article distributed under the terms and conditions of the Creative Commons Attribution (CC BY) license (<http://creativecommons.org/licenses/by/4.0/>).